Morphological and functional characterization of the oyster Crassostrea gasar circulating hemocytes: Cell types and phagocytosis activity

Jesarela Merabe Silva Freire, Natanael Dantas Farias, Hélène Hégaret, Patricia Mirella da Silva

Morphological and functional characterization of the oyster *Crassostrea gasar* circulating hemocytes: cell types and phagocytosis activity.

Jesarela Merabe Silva Freire[a], Natanael Dantas Farias[a], Hélène Hégaret[b], Patricia Mirella da Silva[a]*

[a]Departamento de Biologia Molecular, Centro de Ciências Exatas e da Natureza, Universidade Federal da Paraíba – Campus I, 58051-900, João Pessoa, PB, Brazil. jesarela-msf@hotmail.com; natan.cbio@gmail.com; mirella_dasilva@hotmail.com

[b]Laboratoire des Sciences de l'Environnement Marin LEMAR-UMR6539, Institut Universitaire Européen de la Mer, Université de Bretagne Occidentale, Place Copernic, Technopôle Brest-Iroise, 29280 Plouzané, France. helene.hegaret@univ-brest.fr

*Corresponding author

Departamento de Biologia Molecular, Centro de Ciências Exatas e da Natureza, Universidade Federal da Paraíba – Campus I, 58051-900, João Pessoa, PB, Brazil

mirella_dasilva@hotmail.com

ABSTRACT

Hemocytes are the circulating cells of the hemolymph of oysters and are responsible for numerous physiological functions, including immune defense. The oyster *Crassostrea gasar* is a native species inhabiting mangrove habitat and is of great commercial interest, cultured throughout the Brazilian coast, mainly in the north and northeast. Despite its commercial importance, little is known about its immunological aspects and defense cells, the hemocytes. This work aimed to morphologically characterize hemocytes of the oyster *C. gasar* and to study one of the main cellular defense response, phagocytosis, using light microscopy and flow cytometry. The results showed the presence of six hemocyte populations in *C. gasar* hemolymph. These comprise of large and small granulocytes, large and small hyalinocytes, blast-like cells and a rare type classified as vesicular or serous hemocytes. Hyalinocytes were highly abundant and the most heterogeneous cell population, while small granulocytes, along with vesicular hemocytes were the less abundant population. Hemocytes of *C. gasar* oysters demonstrated capabilities to phagocytose three different types of particles tested: zymosan A, latex particles and *Escherichia* coli, indicating a broad defense capacity. The zymosan A were the most engulfed particles, followed by beads, mainly phagocytized by granulocytes, the most phagocytic cells, and finally *E. coli*, which were the least phagocytized. This study is the first characterization of *C. gasar* oyster hemocytes and will support future studies that aim to understand the participation of different hemocyte types in defense responses against pathogens and/or environmental changes.

KEY-WORDS: *Crassostrea gasar*, hemocytes, immunity, morphology, flow cytometry, phagocytosis, neutral red

1. INTRODUCTION

Studying the immune system of cultured bivalves is important because these organisms are highly subjected to epizootics due to more stressful conditions, such as high density and frequent handling, which could render animals more susceptible to diseases.

The mangrove oyster *Crassostrea gasar* is cultured in several regions of Brazil, but mainly in the north and northeast coast, as opposed to the culture of the Pacific oysters *C. gigas*, which was established a long time ago and succeed in the colder waters of the south, with an annual production of 2,128 tons (https://sidra.ibge.gov.br/tabela/3940). On the contrary, oyster *C. gasar* is produced in extensive system (Valenti et al., 2021), and only since 2013, when a private hatchery facility for *C. gasar* spat production was installed in the northeast, improvements in annual production were observed, which reached an annual production in 2020 of 320 tons.

The expansion and good development of an oyster culture do not rely exclusively on the supply of spats to oyster farmers, but also on environmental conditions (good water quality), management strategies, and the health of animals, among others (Coen and Bishop, 2015; Rodgers et al., 2019). In fact, one of the main production bottleneck is the occurrence of disease outbreaks (Barbosa Solomieu et al., 2015; Carnegie et al., 2021). In Brazil, the main threat to oysters is the protozoan parasite *Perkinsus* spp. that occurs in almost all culture areas in the northeast region (Brandão et al., 2013; da Silva et al., 2014, 2013; Dantas Neto et al., 2020; Queiroga et al., 2015; Sabry et al., 2013; Scardua et al., 2017) and was recently discovered in the south of Brazil (Luz Cunha et al., 2019). We believe that with the intensification of mangrove oyster production in the northeast, perkinsosis could become a considerable threat.

To handle any sanitary issues in the future, more fundamental knowledge of the immune system of the *C. gasar* is needed. A starting point is to characterize this species immune defense cells, called hemocytes. Most studies investigating hemocytes were carried out in commercial bivalve species, such as *C. virginica, C. gigas, C. madrasensis, C. hongkongensis, Saccostrea glomerata, S. kegaki, Ostrea edulis, O. chilensis, Perna canaliculus* and *Ruditapes* spp. (Aladaileh et al., 2007; Allam et al., 2002; Chang et al., 2005; Donaghy et al., 2009a; Hong et al., 2013; Ittoop et al., 2006; Li et al., 2018; Renault et al., 2001; Rolton et al., 2020). Similarly, in Brazil, the most important commercial bivalve species had their hemocytes characterized and some immune functions studied, including the most cultured brown mussel *Perna perna* (Barracco et al., 1999), the mangrove oyster *C. rhizophorae* (Barth et al., 2005), the scallop *Nodipecten subnodosus* (Schleder et al., 2008), and recently the pearl oyster *Pteria hirundo* (Vieira et al., 2017).

It should be noted that two recent studies applied flow cytometry approach to reanalyze the hemocytes of *P. perna* mussel (Fonseca et al., 2022) and *C. rhizophorae* oyster (Rebelo et al., 2013), which complemented the data on characterization of the hemocytes obtained previously by light microscopy for these species. As a result, additional hemocyte types were described, for example, semigranulocyte was identified in *P. perna,* in addition to the three known types (granulocytes, hyalinocytes and small hyalinocytes) (Barracco et al., 1999); and a hemoblast type was recognized in *C. rhizophorae*, in addition to the two known types (hyalinocytes and granulocytes) (Barth et al., 2005). This highlights the importance of combining flow cytometry and microscopy in the characterization of bivalve hemocytes.

Flow cytometry technique can be useful in determining the intracellular complexity, which is sometimes unnoticed using light microscopy. More importantly, flow

cytometry can be used to rapidly measure several cell parameters in the same animal, due to the small volume of sample required by the instrument. In view of this fact, flow cytometry is a valuable tool for studying hemocyte population changes and cell immunological responses including, phagocytosis, production of reactive oxygen species, fluctuations in enzymatic activities, etc. (Nguyen and Alfaro, 2019). These parameters can be altered in response to environmental changes, such as ocean acidification and warming (Li et al., 2015), hypoxia (Andreyeva et al., 2019; Wang et al., 2014), salinity (Jauzein et al., 2013) contaminants (Renault, 2015), harmful algae (Lassudrie et al., 2020) or in response to infection (Comesaña et al., 2012; Hégaret et al., 2010; Prado-Alvarez et al., 2012; Queiroga et al., 2013). On the other hand, light microscopy enables the comparison and classification of hemocytes types based on morphological characteristics such as cell and nucleus size and cytoplasm projections as well as staining affinities of the intracellular granules. Therefore, the combined uses of flow cytometry and light microscopy have been successfully applied to analyze the morphological characteristics of bivalve hemocytes; as reported in several studies with commercial bivalve species of mussels (Donaghy and Volety, 2011; Parrino et al., 2019; Rolton and Ragg, 2020), clams (Donaghy et al., 2009b; Zeng et al., 2021) and oysters (Allam et al., 2002; Andreyeva et al., 2020; Dang et al., 2012; Donaghy et al., 2009a; Hégaret et al., 2003; Hong et al., 2014; Li et al., 2018; Rolton et al., 2020; Xue et al., 2001).

The goal of the present study was to characterize the hemocytes of *C. gasar*. Hemocytes were first analyzed by light microscopy (using neutral red and Giemsa stains) and flow cytometry, and on a second hand, phagocytosis response of hemocytes against biological and inert particles was estimated.

2. MATERIALS AND METHODS

2.1. Animals and hemolymph sampling

Adult *C. gasar* oysters (> 70 mm) were sampled in a farming at Mamanguape River estuary, Paraíba State, Northeast (NE) Brazil (S06°47'08,2"; WO34°59'46,7").

Hemolymph was withdrawn from each animal via the adductor muscle using a 21G syringe and kept on ice to reduce aggregation or immediately fixed depending on the analyses. Hemolymph was observed under a light microscope (Olympus BX41) for contamination, and samples found to contain any impurities were discarded.

The number of animals used in each assay are specified below.

2.2. Microscopic analyses

Two types of hemolymph preparations were performed to analyze hemocyte types using light microscopy. In the first preparation, hemolymph of 30 oysters was individually dispensed onto a slide positioned on a moistened paper to create a wet chamber and were incubated at room temperature (25 °C) for 5 min to allow the cells to adhere to the glass surface. We previously tested different times (5-30 min) for cell adhesion and we found the 5 min was the best time to prevent hemocyte deformation or degranulation (data not shown). The cell monolayers were fixed with methanol (5 min) and stained with Giemsa (Newprov) (5 min). Hemocytes were analyzed under a light microscope (Olympus BX41) and photographed (Olympus Q-Color 5TM camera). One hundred cells per oyster were characterized based on the Giemsa staining pattern of the intracytoplasmic granules (basophilic or acidophilic), nucleus/cytoplasm ratio, shape (rounded or spread), plasma-membrane protrusions (filipodia or lamellipodia) and size (where the measurement of cell diameter was taken from the largest axis, without

considering cytoplasmic projections). This staining with Giemsa also allowed to identify and quantify hemocyte types and their proportions for each animal.

In the second preparation, fresh hemolymph of 10 different oysters was individually mixed with a vital staining, the neutral red (Sigma-Aldrich, final concentration 0.005%) (Cima and Matozzo, 2018). No measurements of cells were taken, instead hemocytes stained with neutral red were observed adhering on the slide for up to 20 min in order to assess cytoplasmic projections, as well as characteristics of intracytoplasmic vesicles/granules, as neutral red has the ability to cross the plasma membrane of cells and stain acid compartments including lysosomes. Several cells (at least 100 per sample) were analyzed under a phase contrast microscope (Olympus BX41) and photographed (Olympus Q-Color 5TM camera).

2.3. Flow cytometry analyses

Hemolymph from the same 30 oysters used for microscopic analyses (stained with Giemsa) was alongside prepared for flow cytometry. The hemolymph was immediately fixed using cold 4% formaldehyde (final concentration 2%) in filtered sterilized seawater (FSSW) (the efficiency of fixation of this concentration for hemocytes in suspension was previously tested, data not shown) and then, analyzed in the FACSCalibur flow cytometer (BD Biosciences, San Jose, California, USA). Hemocyte populations were discriminated in forward scatter (FSC) *vs* side scatter (SSC) cytograms, representing proxies of the size and internal complexity (an indicator of intracytoplasmic granules), respectively.

2.4. Phagocytosis assays

Three different particles were used to estimate the phagocytic activity of hemocytes (García-García et al., 2008; Prado-Alvarez et al., 2012): Fluorescent latex beads (Fluoresbrite yellow-green microspheres, 2µm, Polysciences), zymosan A (Texas Red conjugate, ~ 3µm, Life Technologies) and *Escherichia coli* (Texas Red conjugate, ~1µm, Life Technologies). Particles were diluted in phosphate buffer to a final concentration of 1×10^6 mL^{-1}.

Hemolymph from each oyster (n = 30) was dispensed into three tubes each containing a type of particle suspension having a ratio of 1:10, hemocyte: particles. Hemolymph with FSSW alone was used as a control (García-García et al., 2008; Prado-Alvarez et al., 2012). Hemolymph was incubated for 1h at 25°C, and then analyzed in a flow cytometer.

Hemocyte populations were first selected in FSC *vs* SSC dot plot cytogram to be visualized in SSC *vs* fluorescence cytograms; green (530 nm) for latex beads and red (613 nm) for zymosan A and *E. coli*. Phagocytosis was estimated in a fluorescence histogram by selecting peaks of hemocytes engulfing particles (adapted from Hégaret et al., 2003a), i.e. hemocytes which appeared fluorescent (as opposed to non-fluorescent, non-phagocytic hemocytes). Therefore, all fluorescent hemocytes were considered engulfing and total phagocytosis was estimated. Microscopic observations were performed in order to confirm that particles (beads, zymosan and bacteria) were actually engulfed and not just bound to the membranes or attached to cell surface of hemocytes.

2.5. Statistical analyses

D'Agostino & Pearson normality test was applied to all data. For percentage data, an arcsine square root transformation was used. Kruskal-Wallis followed by Dunns

post-hoc test was used to compare hemocyte size by light microscopy and flow cytometry.

One-way ANOVA followed by a Tukey post-hoc test was used to compare phagocytosis of beads, zymosan A and *E. coli* for total hemocyte population. The unpaired t-test was used to compare the phagocytic capacity of *E. coli* and latex phagocytosis (separately) between granulocytes and hyalinocytes.

Differences were considered significant when $p \leq 0.05$. Data were expressed as mean ± standard error (SE). Statistical analyses were performed using the Statgraphics Centurion XV software.

3. RESULTS

3.1. Morphological characterization of *C. gasar* hemocytes by light microscopy

Oyster hemolymph presented six populations with different size, morphology, and staining properties: large (LG) and small (SG) granulocytes, large (LH) and small hyalinocytes (SH), blast-like cells (BL) and a sixth rare type, which we identified as either vesicular or serous hemocytes (V).

LG were the largest cell type among *C. gasar* hemocyte populations (31.5 ± 0.31 µm; **table 1**) with a low nucleus/cytoplasm ratio. The nucleus was rounded and eccentric. The cytoplasm contained many small acid granules, stained red (neutral red) or blue (Giemsa). These cells quickly projected filipodia and lamellipodia in spontaneous adhesion (**Figs. 1a-b**) and comprised 14.4% (± 1.48) of the total hemocyte population (**Table 1**).

Table 1. Size and proportion of hemocytes in the hemolymph of *C. gasar* (n = 27), obtained by light microscopy (LM) and flow cytometry (FC). Values are mean ± SE. n: number of hemocytes analyzed by LM (Giemsa staining). FSC: forward scatter.

	µm (LM)	n	A.U. (FSC, FC)	% (LM)	% (FC)
Large Granulocytes (LG)	31.5 ± 0.31**a**	694	369.5 ± 12.96 **a**	14.4 ± 1.48	6.3 ± 0.79
Small Granulocytes (SG)	11.9 ± 0.22 **c**	282	160.3 ± 4.32 **b**	4.8 ± 1.05	1.3 ± 0.15
Large Hyalinocytes (LH)	23.4 ± 0.32 **b**	494	303.1 ± 2.34 **a**	30.4 ± 1.58	38.2 ± 2.13
Small Hyalinocytes (SH)	10.7 ± 0.13 **c**	529	138.7 ± 2.3 **b**	33.0 ± 1.85	43.8 ± 1.85
Blast-like cells (BL)	5.4 ± 0.06 **d**	489	43.55 ± 0.35 **c**	16.0 ± 1.91	10.6 ± 1.24
Vesicular/Serous cells (V)	22.7 ± 0.26	34	No data	1.3 ± 0.45	No data

Different letters denote significant differences in size among the hemocyte types (separately for each technique), $p < 0.0001$, Dunns post-hoc test. Vesicular/serous cells were not included in statistical analyses because they were not distinguished by FC.

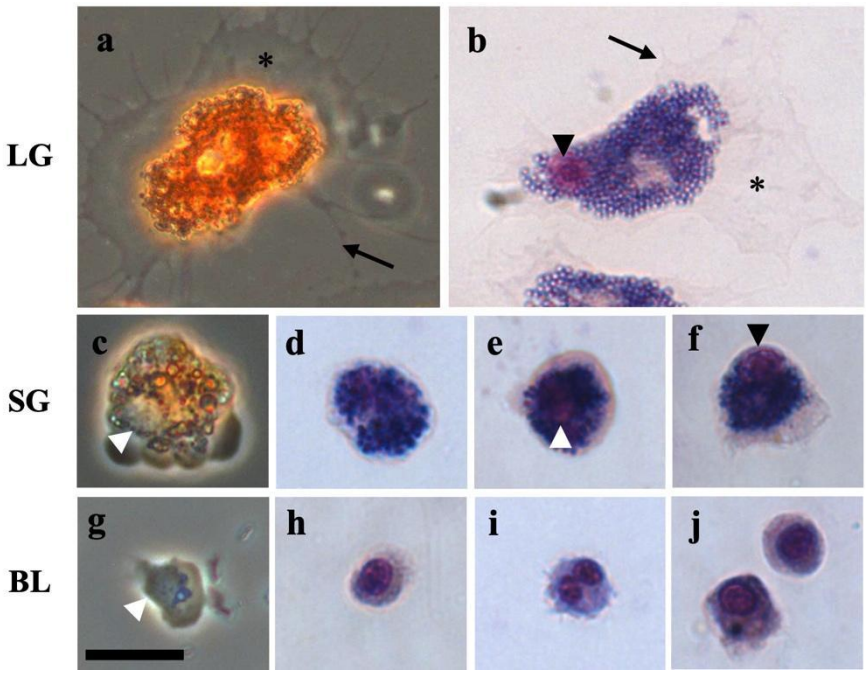

Fig. 1. Hemocytes from *C. gasar* hemolymph stained with neutral red (a, c, g, phase contrast) and Giemsa (b, d-f, h-j, bright field). LG (Lager granulocytes), small granulocytes (SG) and blast-like cells (BL). Note a binuclear cell in i. Cytoplasmic projection filipodia and lamellipodia (arrows), ectoplasm (*), endoplasm containing several red or blue (basophilic) granules and the nucleus (arrowheads). Bar = 10 ⌈m for all images.

SG showed a medium size of 11.9 µm ± 0.22 (**Table 1**) low nucleus/cytoplasm ratio. The nucleus was rounded or oval and eccentric, and the cytoplasm contained large and abundant granules stained red (neutral red) or blue (basophilic, Giemsa) (**Figs. 1c-f**). In SG, the granules almost completely covered the nucleus and had minimal cytoplasmic projections. They were the least abundant cell type in the hemolymph (4.8% ± 1.05; **table 1**).

BL cells were the smallest cells (5.4 µm ± 0.06; **table 1**), with a high nucleus/cytoplasm ratio and eccentric nucleus, sometimes no cytoplasmic projections. BL cells had highly basophilic cytoplasm without granules or prominent membrane projections (**Figs. 1g-j**).

The hyalinocytes were the most numerous and heterogeneous hemocyte population in the hemolymph (**Table 1**). Two main types were identified: small (SH) and large (LH) hyalinocytes in the following proportions, 33.0% ± 1.85 and 30.4% ± 1.58, respectively.

The SH were similar in size to small granulocytes (10.7 µm ± 0.13; **table 1**). They presented a high nucleus/cytoplasm ratio and had rounded or elongated large nucleus which was mostly centered. SH showed lightly basophilic cytoplasm which was often without granules. Cytoplasm projections were scarce and often thick when present (**Figs. 2a-d**).

The LH were the second-largest cell type (23.4 µm ± 0.32; **table 1**), after LG. LH had a low nucleus/cytoplasm ratio, central or eccentric nucleus, and the cytoplasm was lightly acidophilic with few unstained granules, which would have been unnoticed if not observed under a phase-contrast (**Fig. 2e**). LH quickly produced variable types of cytoplasm projections, from thick and long to thin and short (**Fig. 2f**).

The V hemocytes were as large as (22.7 µm ± 0.26; **table 1**) LH and rarely observed (1.3% ± 0.45). They were characterized as rounded cells with a low nucleus/cytoplasm (N/C) ratio, central or eccentric nucleus with mainly lamellipodia projections and few filipodia (**Fig. 2g**). They presented an endoplasm that contained few granules and vacuoles of irregular size and shape that stained blue (basophilic), although some did not stain (**Figs. 2h-i**).

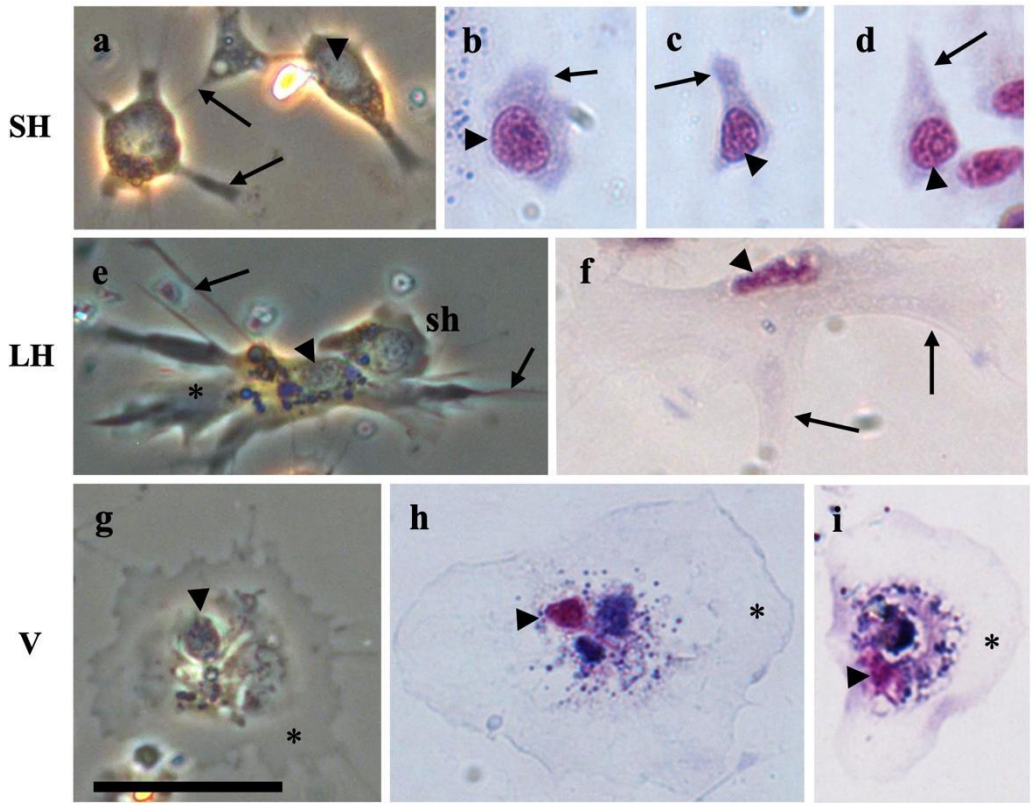

Fig. 2. Hemocytes from *C. gasar* hemolymph stained with neutral red (a, e, g, phase contrast) and Giemsa (b-d, f, h-i, bright field). Small hyalinocytes (SH), large hyalinocytes (LH) and vesicular cells (V). Nucleus and cell sizes can be comparing

between SH and LH in picture e where both are aside. Note endoplasm lacking or containing few unstained granules in hyalinocytes or irregular bluish (basophilic) vacuoles in vesicular/serous cells. Cytoplasmic projections and lamellipodia (arrows), ectoplasm (*) and the nucleus (arrowheads). Bar = 20 ⌈m for all images.

3.2. Morphological characterization of *C. gasar* hemocytes by flow cytometry

Five hemocyte populations were detected in the FSC *vs* SSC cytograms describing cell morphological characteristics from fixed hemolymph of *C. gasar* (**Fig. 3**). Type 1 comprised hemocytes with the lowest size and internal complexity; type 2 was higher in size and internal complexity with more granularity than type 1 but lower than type 3. Type 3 was hemocytes with medium variable size and complexity; types 4 and 5 were hemocytes with the highest complexity and variable sizes.

There were statistical differences in size between the hemocyte types, and these differences were similar in each technique; LH and LG were the highest types, SH and SG were median cells and BL were the smallest in both techniques (**Table 1**). The proportions of hemocyte types were also very similar. Small and large hyalinocytes were the most numerous cells in the hemolymph, and in contrast, the small granulocytes were less abundant (**Table 1**). Thus, it could be inferred that BL, SH, LH, LG and SG would correspond to types 1, 2, 3, 4 and 5, respectively.

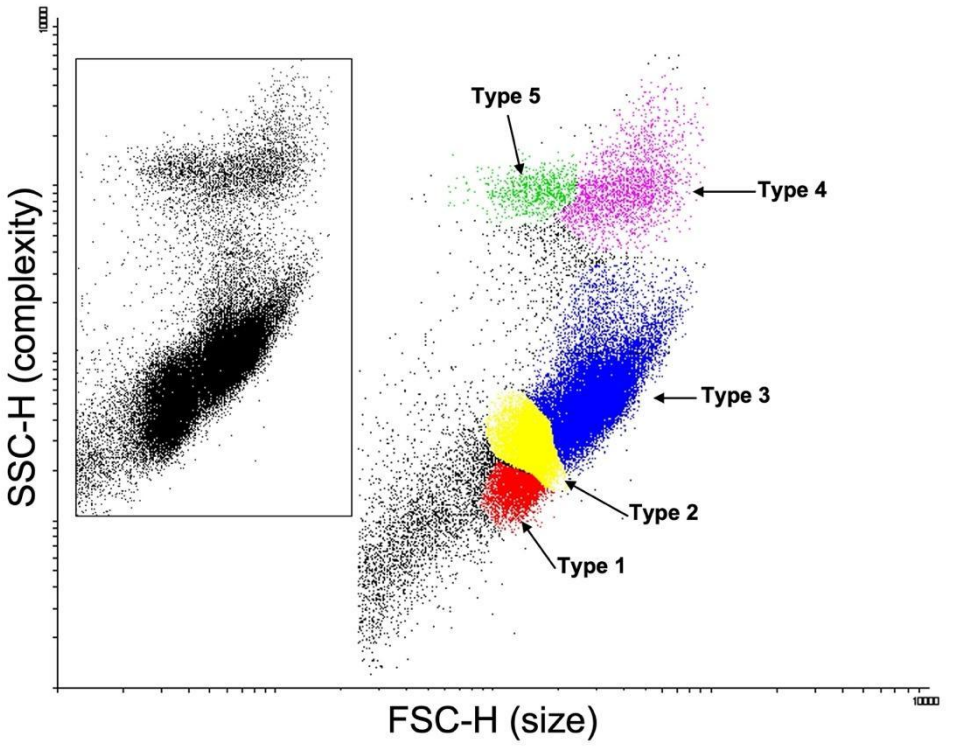

Fig. 3. Representative forward scatter (FSC, size) *vs* side scatter (SSC, complexity) cytogram of formaldehyde-fixed *C. gasar* hemolymph. Regions were drawn around the five main populations of hemocytes visualized and dense groups of dot (cells) and are showed by colors and labelled as: type 1 (BL); type 2 (SH); type 3 (LH); type 4 (LG) and type 5 (SG). Vesicular hemocytes (V) would be within type 3. Inset represents the same cytogram without delineation of regions representing the hemocytes populations.

3.3. Phagocytosis of different fluorescent particles

Hemocytes of *C. gasar* oysters were capable of engulfing the three distinct types of particles tested: inert latex fluorescent beads (**Figs. 4a-b**) and biological fluorescent bacteria *E. coli* (**Figs. 4c-d**) and yeast particles of zymosan A (**Figs. 4e-f**).

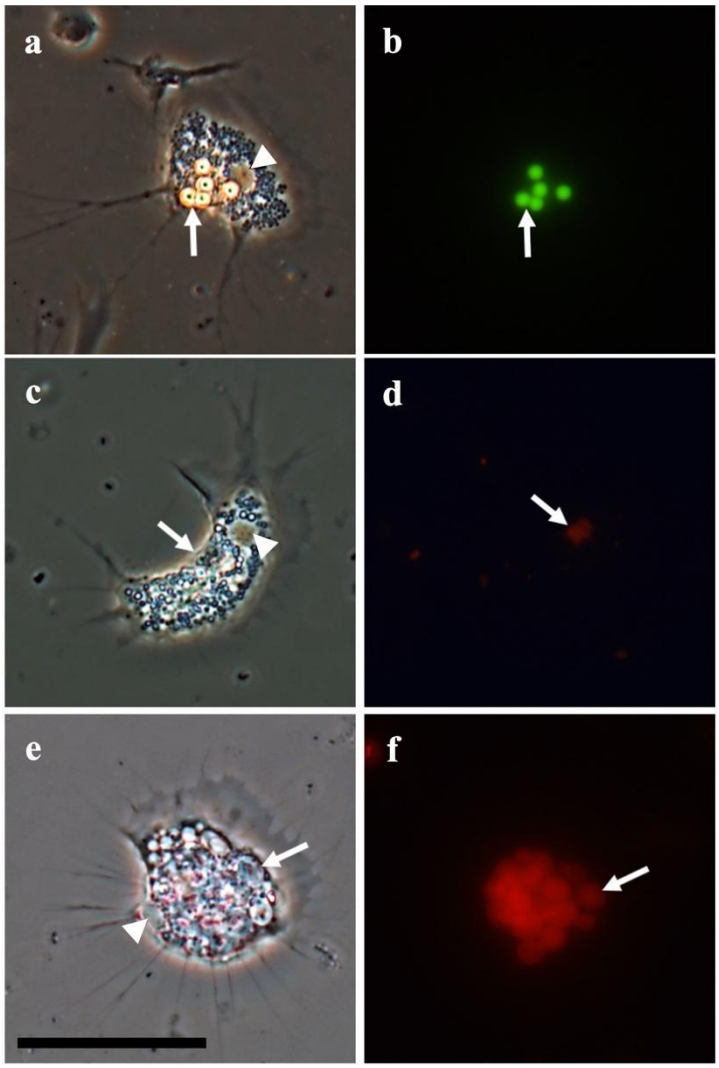

Fig. 4. Phagocytosis of different particles by *C. gasar* hemocytes. Images from phase contrast (left) and fluorescence (right) microscope. a-b. Latex beads (green-fluorescence); c-d. *E. coli* (red-fluorescence). e-f. Zymosan A (red-fluorescence). Note the particles inside the cytoplasm of the hemocytes (arrows) and the small size of *E. coli* compared to zymosan A and latex beads. Occasionally zymosan A were observed to thicken. Nucleus (arrowhead) are identified on each light microscopy picture (**a, c, e**). Bar = 20 ⌈m for all images.

Latex beads phagocytosis activity was analyzed in individual hemocyte populations, granulocytes *vs* hyalinocytes, since peaks of fluorescence were well defined (**Fig. 6**

a). For *E-coli* and zymosan particles, peaks were not observed in fluorescence histograms (**Figs. 5c -d**), instead a slight increase of fluorescence was detected for *E. coli* indicating a very low phagocytic rate. For zymosan, a high increase of fluorescence was noticed despite no clear peak observed, but a *plateau*, presumably due to the irregular shape of zymosan particles. Thus, to not overestimate or underestimate the phagocytosis for separate granulocytes and hyalinocytes populations, phagocytosis was estimated for total population of hemocytes (**Fig. 7 a**).

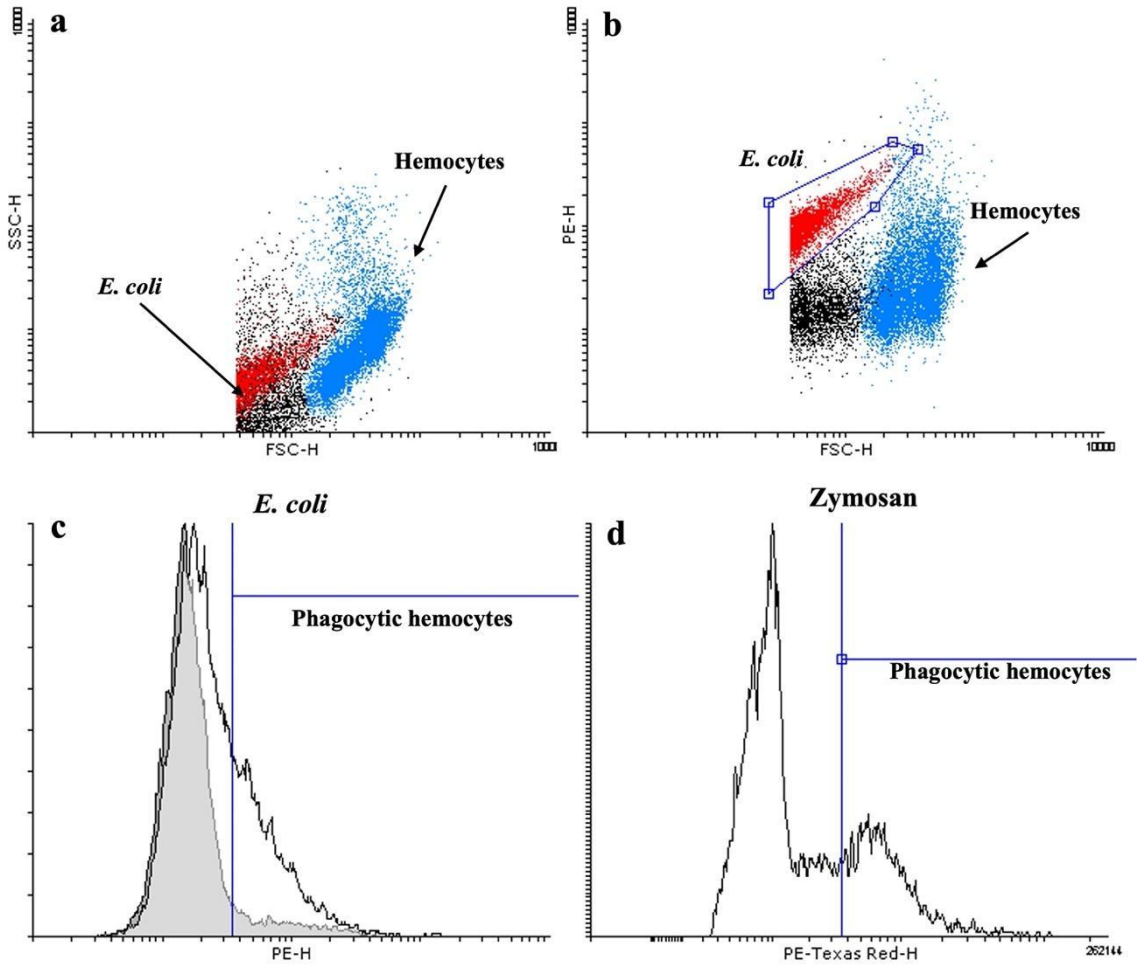

Fig. 5. Representative flow cytometry graphics of phagocytosis of *E. coli* and zymosan by *C. gasar* hemocytes. **a**. Total population of hemocytes selected (blue) on FSC vs SSC dot plot; **b.** Red fluorescence vs FSC dot plot allowed to visualize free-fluorescent particles *E. coli* or zymosan (red) and select them. **c.** Phagocytosis of

fluorescent *E. coli* was estimated by gating hemocytes and excluding (gate off) *E. coli* from the histogram. The histogram shows the slight increase of the fluorescence represented by phagocytic hemocytes (white in the overlay histogram) compared with non-phagocytic cells. Total fluorescence of hemocytes with particles was diminished from the control (hemolymph without particles); **d.** Phagocytosis of fluorescent zymosan was estimated similarly on the histogram.

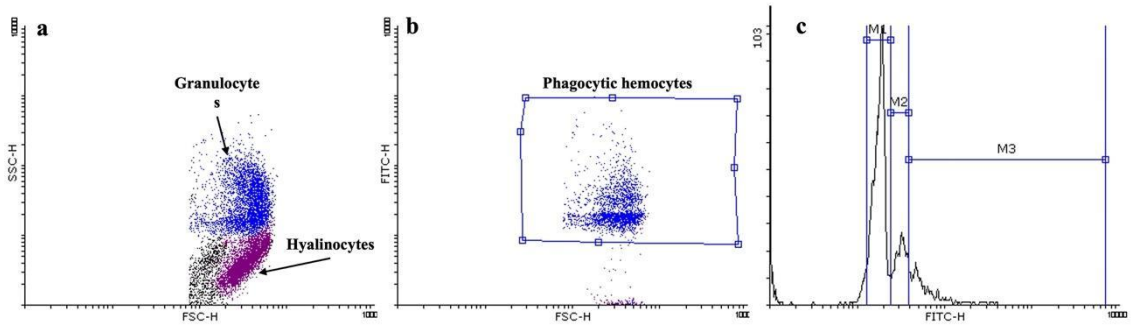

Fig. 6 . Representative flow cytometry graphics of phagocytosis of latex beads by *C. gasar* hemocytes. **a.** Granulocytes and hyalinocytes selected on FSC vs SSC dot plot; **b.** Gated hemocytes on green fluorescence vs FSC dot plot; **c.** Gated hemocytes on green fluorescence histogram showing peaks of hemocytes engulfed 1 bead (M1), 2 beads (M2) and > 3 engulfed beads (M3), the latter were used for to determine % of phagocytic hemocytes.

Hemocytes showed different phagocytic abilities to the different particles. Zymosan A was the most phagocytosed particle, followed by latex beads and *E. coli* (**Fig. 7 a**). Granulocytes were significantly more phagocytic than hyalinocytes (**Fig. 6b and 7b**). BL cells did not phagocyte which was also confirmed observing the preparations under microscope.

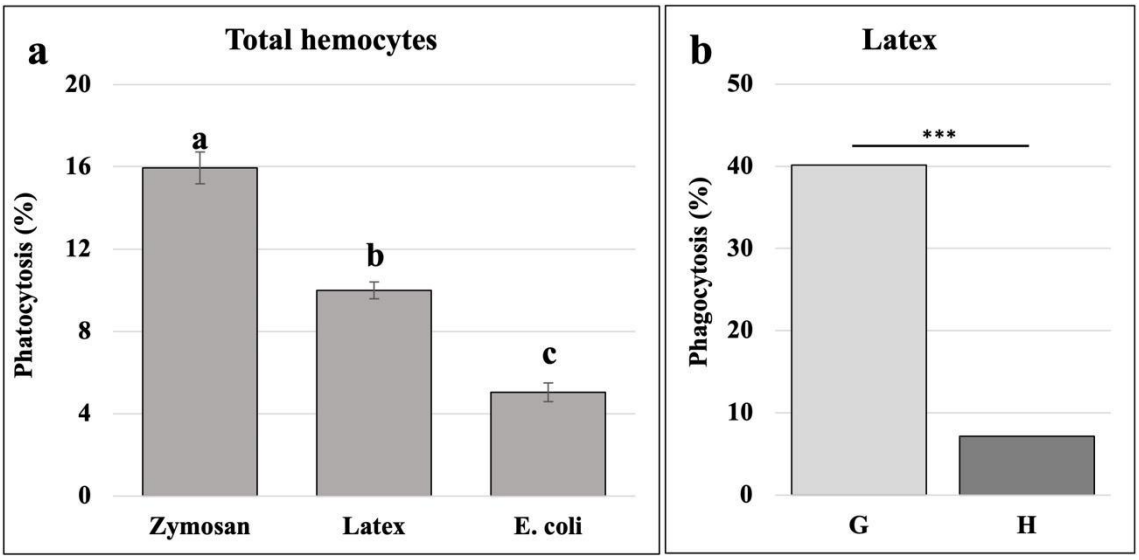

Fig. 7 . Phagocytosis (%) of different particles by *C. gasar* hemocytes. **a**. Total hemocytes population. Different letters denote significant differences (ANOVA, $p < 0.0001$, Tukey post-hoc test). **b.** Latex phagocytosis (> 3 beads) by granulocytes (G) and hyalinocytes (H) populations (including large and small subtypes). *** Significant differences (*t*-test, $p < 0.0001$). n = 30 oysters.

4. DISCUSSION

The present work is, to our knowledge, the first morphological and functional characterization of hemocytes of mangrove oyster *C. gasar*. Based on light microscopy and flow cytometry analyses, six hemocyte populations were identified in the hemolymph: large and small granulocytes, large and small hyalinocytes, blast-like cells, and a rare type of hemocytes, which we identified as either vesicular or serous hemocytes. The recent review of de la Ballina et al. (2022) highlights the distinct composition in hemocyte types of the hemolymph of different species of bivalves. However, in a global classification three main types (granulocytes, hyalinocytes and

blast-like cells) are found, which are easily distinguishable by light microscopy and flow cytometry.

The morphometry (N/C ratio and cell size) and tinctorial properties of *C. gasar* hemocytes observed herein were compatible with those reported in bivalves and specially oysters species (de la Ballina et al., 2022). Large and small granulocytes were cells with granules within the cytoplasm (blue or red, according to the stain) and a low N/C ratio, and hyalinocytes had few or no granules and a higher N/C ratio. Blast-like cells exhibited the highest N/C ration and were the smallest cell. In terms of plasma membrane projections, LG and LH of *C. gasar* quickly projected filipodia and lamellipodia, suggesting the possibility that they might be involved in more dynamic function, such as phagocytosis process that requires fast migration and adhesion, making them frontline cells of the oyster innate immune system. Filipodia are thin cytoplasmic protrusions that sense and explore the surrounding environment and act as tentacles attracting particles; while lamellipodia, wave-like extensions, are major structures in cell motility, allowing, for instance, neutrophils migrate towards a chemoattractant (Mattila and Lappalainen, 2008). SG, SH and BL of *C. gasar* did not exhibit protrusions, suggesting they might be associated with other functions or represent an intermediate stages of maturation/differentiation, as already proposed by several authors, but still controversial (see review of de la Ballina et al., 2022).

Concerning the proportion of each hemocyte type in the hemolymph of *C. gasar*, in general, it reflected previous studies in other oysters species such as *Crassostrea* spp. (Allam et al., 2002; Chang et al., 2005; Donaghy et al., 2009a; Hong et al., 2014; Li et al., 2018; Rebelo et al., 2013), *Saccostrea* spp. and *Ostrea* spp. (Aladaileh et al., 2007; Hong et al., 2013; Rolton et al., 2020; Xue et al., 2001). In both techniques applied here, hyalinocytes constituted the most abundant hemocyte population in *C. gasar*

hemolymph, whilst small and large granulocyte populations combined occurred in similar proportion as blast-like cells and the vesicular hemocytes were the least detected and only by LM. Small granulocytes were not observed in all specimens studied. This fact was previously noticed in the hemolymph of *C. virginica*, *O. edulis* and *S. glomerata*, when number of specimens studied was low; three, eight and five, respectively. Accordingly, some differences in the hemocyte types observed inter and intra bivalve's species detected by flow cytometry might be related to sample preparation. Noted that small and large hyalinocytes appeared as one merged population in fresh samples instead of two in formaldehyde-fixed hemolymph of *C. virginica*. Indeed, live and active cells undergo morphological changes to perform their functions or respond to stimuli, and therefore, distinguishing populations with subtle morphological differences is difficult.

Hyalinocytes (small and large) of *C. gasar* presented a wide variety of forms, when observed under a microscope, which was also detected by flow cytometry. This suggests a potential diversity of hyalinocyte activities, with is in accordance with the wide range of functions these cells can perform to carry out the physiological responses, beside immunological roles, such as transport of nutrients, excretion, shell formation, and reproduction (Cheng, 1996; de la Ballina et al., 2022).

Granulocytes of *C. gasar* contained abundant granules, which were tiny in large granulocytes and big in small granulocytes, representing two distinct subpopulations. The granules were exclusively basophilic, indicating a predominance of acid content evidenced by the neutral red staining. Indeed, granulocytes are rich in intracytoplasmic granules, including lysosomes, an acid compartment containing hydrolytic enzymes, which play a key role in the digestion of phagocytosed microorganisms (Allam and Raftos, 2015). On the contrary, some species of oysters *Crassostrea* and *S. glomerata*

have granulocytes containing eosinophilic granules or basophilic granules or a combination of both (Aladaileh et al., 2007; Chang et al., 2005; Ittoop et al., 2006; Rebelo et al., 2013). Moreover, mix of basophilic and refringent granules were described in *C. ariakensis* (Donaghy et al., 2009a). The chemical composition of these granules is certainly distinct (Friebel and Renwrantz, 1995) and it could be related to different cell function. It has been reported that acidophilic granulocytes have more enzymes and phagocytic capacity than basophilic granulocytes, which granules would still mature (Cheng, 1996; de la Ballina et al., 2022).

Blast-like hemocytes of *C. gasar* had features of undifferentiated cells, with eventually had a binucleated nucleus, which might suggest rapid BL hemocyte proliferation. Hemoblasts with the same binucleated nucleus feature were reported in the hemolymph of *R. philippinarum* and were considered in mitosis (telophase) (Cima and Matozzo, 2018). Morphologically hemoblasts correspond to blast-like cells. The authors observed hemoblasts in different mitotic phases, which according to the study represented hemocyte proliferation in response to *E. coli* challenge. Liu and Zhao (2018) also detected bi and trinucleated granulocytes and hyalinocytes besides other polymorphonuclear hemocytes. In *C. gasar* an increase in the BL population was induced by *Perkinsus* spp. infection (Queiroga et al., 2013), although the authors have not made observations of the cells under the microscope to ascertain the presence of mitotic figures.

A remarkably and scarce hemocyte type found in the hemolymph of *C. gasar* had some characteristics, such as: large cells with low N/C ration and presence of vesicles and vacuoles suggesting degranulation, that would suggest they are vesicular hemocytes, which were detected in the hemolymph of some oyster's species. In *O. edulis*, these cells were described as degranulated hemocytes (Auffret, 1989), in *C.*

gigas, devoided of granules but with lucent vacuoles (Chang et al., 2005), and in *S. kegati* vacuolated granulocytes (Hong et al., 2013). In other bivalves, they were also described by containing vacuolated cytoplasm or with abundance of clear vesicles and a lack or scarcity of cytoplasmic granules (Preziosi and Bowden, 2016; Salimi et al., 2009). Nevertheless, no function of vesicular hemocytes has been enlightened so far.

The remarkably hemocyte type found here, projected lamellipodia, suggesting a migration ability. Thus, we suspected they might play a role in tissue repairs via diapedesis, removal of debris and injured host cells resulting from pathological processes (Carella et al., 2015). Indeed, their cytoplasm also contained abundance of irregular (in shape and staining features - metachromasia) vesicles, presumably holding different chemical natures materials, which supports a degradative function (Carella et al., 2015). In this sense, we also suggest that, it could be serious cells, a polemic cell type found in tissues and in low amount in hemolymph of some bivalves (de la Ballina et al., 2022), which are able to perform diapedesis and are likely involved in degradation and detoxification process (de la Ballina et al., 2022; Hine, 1999). In the hemolymph of *R. philippinarum* serous cells are found in low proportion (1%) (Cima et al., 2000), similar to in the current study (1,3%) and an increase in the number of serous cells was detected after *E. coli* challenge (Cima and Matozzo, 2018). The morphological characteristics of vesicular and serous cells described in the literature can be easily confused, since both have presence of large vacuoles. A study aiming to verify the proportion of these cells in the hemolymph of infected *C. gasar* would help to clarify this issue.

In the current study, we also investigated the phagocytosis activity of *C. gasar* hemocytes using different particles. Phagocytosis is the main defense response against non-self-particles, which can be triggered by small-sized parasites or can be inhibited or

potentiated by an infectious agent (Allam and Raftos, 2015), as demonstrated in *C. gasar* infected by *Perkinsus* sp. Our data show that zymosan and latex beads were the most phagocytosed particles compared to *E. coli* bacteria. This demonstrates, on one hand, that hemocytes of *C. gasar* can recognize non-self-molecules, such as fungi and bacteria, as well as inert particles (latex fluorescent beads). Our study also demonstrates differences in phagocytosis rate of the different particles, which could either be attributable to their size or to their chemical composition, indeed, larger biological particles (zymosan) were more engulfed than inert particles. This result differed from other studies, where hemocytes engulfed a similar or higher amount of latex beads than zymosan, such as in the mussel *Mytilus galloprovincialis* (García-García et al., 2008) and, the clam *R. decussatus* (Prado-Alvarez et al., 2012). In both the latter studies, *E. coli* was the lowest engulfed particle. *Vibrio alginolyticus* was the most phagocyted by *M. galloprovinciallis* hemocytes, when compared with latex beads or zymosan (García-García et al., 2008). The lowest phagocytosis of *E. coli* particles by hemocytes may be related to its non-pathogenicity to bivalves. Indeed, one study in *C. gigas* hemocytes found that recognition and phagocytosis differ according to *Vibrio* spp. (Zhang et al., 2014). Moreover, the authors observed that *V. splendidus* induced a specific enhancement of phagocytosis after a secondary challenge.

Despite six morphologically distinct populations of hemocytes were detected, it was not possible to quantify phagocytosis for all of them, since they were not totally distinguished by FC or even by LM, probably due to the cellular modification that cells undergo after 1h of incubation with the fluorescent particles. However, for latex particles, two main populations could be differentiated, granulocytes and hyalinocytes, and phagocytosis analyzed, although not in terms of their subpopulations (small and larger). It was possible to confirm that BL cells were not phagocytic. Probably due to its

low oxidative activity and low lysosomal content (Evariste et al., 2016). Donaghy et al. (2009a) also found that *C. ariakensis* blast-like cells did not show any phagocytosis or oxidative activity.

Granulocytes engulfed more latex beads than hyalinocytes. This result is consistent with other studies. It has been shown that granulocytes are the most phagocytic hemocyte in mussels (Donaghy and Volety, 2011; García-García et al., 2008), clams (Donaghy et al., 2009b) and oysters (Dang et al., 2012; Donaghy et al., 2009a; Hégaret et al., 2003; Hong et al., 2014). In *R. decussatus*, all hemocytes types (granulocytes, hyalinocytes and intermediate cells) engulfed more latex beads than *E. coli* or zymosan (Prado-Alvarez et al., 2012). Differences in phagocytosis of zymosan, latex beads, *V. alginolyticus* and *E. coli*, between hemocyte types were also reported for *M. galloprovinicialis* (García-García et al., 2008). The large granular cells, that would potentially correspond to granulocytes, engulfed more *E. coli* (9%) than the two semigranular hemocyte populations (large, 5% and small, 0.7%).

Hemocytes perform numerous physiological and immunological functions, therefore, monitoring them can represent *a proxy* for animal health. Changes in total hemocyte counts, proportion of hemocyte types and phagocytosis capacity have been previously used for this purpose (Barracco and Da Silva, 2008; Fournier et al., 2000; Renault, 2015). These hemocyte parameters vary seasonally (Donaghy et al., 2009b) in response to infection (Da Silva et al., 2008; Queiroga et al., 2013) and susceptibility to diseases (Comesaña et al., 2012) and in response to different environmental conditions (Andreyeva et al., 2020; Lassudrie et al., 2020; Li et al., 2015; Renault, 2015; Xie et al., 2021). Thus, the knowledge of hemocyte types of *C. gasar* will be helpful to understand the impact of parasites and environmental conditions of oysters cultured in estuaries on the Brazilian coast.

5. CONCLUSIONS

This study, combining flow cytometry and light microscopy succeeded in classifying the hemocyte types of *C. gasar* hemolymph into six populations, with two subtypes of granulocytes and hyalinocytes (small and large), a blast-like cell and a less abundant type (vesicular/serous cell), which function is likely associated with tissue repairs during pathological process. Both granulocytes and hyalinocytes, probably the large subtypes of both, are the frontline cells of the oyster innate immune system engulfing and degrading different kind of particles. The knowledge on *C. gasar* hemocytes will facilitate the proposition of new studies aiming at understanding its role in the immune response of the oyster.

CRediT author statement

Jesarela Merabe Silva Freire: Analysis and interpretation of data. **Natanael Dantas Farias**: Writing - original draft. **Patricia Mirella da Silva**: Conceptualization and writing - review & editing, funding acquisition.

Declaration of competing interest

The authors declare that they have no known competing financial interests or personal relationships that could have appeared to influence the work reported in this paper.

ACKNOWLEDGEMENTS

Funding: This work was supported by the *Conselho Nacional de Desenvolvimento Científico e Tecnológico*, CNPq, Brazil [409277/2021-5]; *Fundação*

de Apoio a Pesquisa do Estado da Paraíba, FAPESQ [EDITAL No 09/2021 Demanda Universal], 3046/2021; the public call n. 03 *Produtividade em Pesquisa* [PROPESQ/PRPG/UFPB/PVA13270-2020]; the Conchologists of America [COA Grant to Malacology 2021]. PMS was granted with a CNPq Productivity Fellowship [306721/2021-0].

REFERENCES

Aladaileh, S., Nair, S. V, Birch, D., Raftos, D.A., 2007. Sydney rock oyster (*Saccostrea glomerata*) hemocytes: Morphology and function. J. Invertebr. Pathol. 96, 48–63. https://doi.org/10.1016/j.jip.2007.02.011

Allam, B., Ashton-Alcox, K.A., Ford, S.E., 2002. Flow cytometric comparison of haemocytes from three species of bivalve molluscs. Fish Shellfish Immunol. 13, 141–158. https://doi.org/10.1006/fsim.2001.0389

Allam, B., Raftos, D., 2015. Immune responses to infectious diseases in bivalves. J. Invertebr. Pathol. 131, 121–136. https://doi.org/10.1016/j.jip.2015.05.005

Andreyeva, A.Y., Efremova, E.S., Kukhareva, T.A., 2019. Morphological and functional characterization of hemocytes in cultivated mussel (*Mytilus galloprovincialis*) and effect of hypoxia on hemocyte parameters. Fish Shellfish Immunol. 89, 361–367. https://doi.org/10.1016/j.fsi.2019.04.017

Andreyeva, A.Y., Kladchenko, E.S., Vyalova, O.Y., Kukhareva, T.A., 2020. Functional Characterization of the Pacific Oyster, *Crassostrea gigas* (Bivalvia: Ostreidae), Hemocytes Under Normoxia and Short-Term Hypoxia. Turkish J. Fish. Aquat. Sci. 21, 125–133. https://doi.org/10.4194/1303-2712-v21_3_03

Auffret, M., 1989. Comparative study of the hemocytes of two oyster species: the European flat oyster, *Ostrea edulis*, Linnaeus, 1750 and the Pacific oyster

Crassostrea gigas (Thunberg,1793). J. Shellfish Res. 8, 367–373.

Barbosa Solomieu, V., Renault, T., Travers, M., 2015. Mass mortality in bivalves and the intricate case of the Pacific oyster, *Crassostrea gigas*. J. Invertebr. Pathol. 131, 2–10. https://doi.org/10.1016/j.jip.2015.07.011

Barracco, M., Da Silva, P., 2008. Hemolinfa e sistema imune. O Mexilhão Perna perna 85–103.

Barracco, M., Medeiros, I., Moreira, F., 1999. Some haemato-immunological parameters in the mussel *Perna perna*. Fish Shellfish Immunol. 9, 387–404. https://doi.org/10.1006/fsim.1998.0196

Barth, T., Moraes, N., Barracco, M.A., 2005. Evaluation of some hemato-immunological parameters in the mangrove oyster *Crassostrea rhizophorae* of different habitats of Santa Catarina Island, Brazil. Aquat. Living Resour. 18, 179–186. https://doi.org/10.1051/alr:2005019

Brandão, R.P., Boehs, G., Sabry, R.C., Ceuta, L.O., Luz, M.D.S.A., Queiroga, F.R., da Silva, P.M., 2013. *Perkinsus* sp. infecting oyster *Crassostrea rhizophorae* (Guilding, 1828) on the coast of Bahia, Brazil. J. Invertebr. Pathol. 112, 138–141. https://doi.org/10.1016/j.jip.2012.11.003

Carella, F., Feist, S.W., Bignell, J.P., De Vico, G., 2015. Comparative pathology in bivalves: Aetiological agents and disease processes. J. Invertebr. Pathol. 131, 107–120. https://doi.org/10.1016/j.jip.2015.07.012

Carnegie, R.B., Ford, S.E., Crockett, R.K., Kingsley-Smith, P.R., Bienlien, L.M., Safi, L.S.L., Whitefleet-Smith, L.A., Burreson, E.M., 2021. A rapid phenotype change in the pathogen *Perkinsus marinus* was associated with a historically significant marine disease emergence in the eastern oyster. Sci. Rep. 11, 12872. https://doi.org/10.1038/s41598-021-92379-6

Chang, S., Tseng, S., Chou, H., 2005. Morphological characterization via light and electron microscopy of the hemocytes of two cultured bivalves: A comparison study between the hard clam (*Meretrix lusoria*) and Pacific oyster (*Crassostrea gigas*). Zool. Stud.

Cheng, T.C., 1996. Hemocytes: forms and functions, in: Kennedy, V.S., Newell, R.I.E., Eble, A.F. (Eds.), The Eastern Oyster: Crassostrea Virginica. Maryland Sea Grant, College Park, MD, USA, pp. 299–333.

Cima, F., Matozzo, V., 2018. Proliferation and differentiation of circulating haemocytes of *Ruditapes philippinarum* as a response to bacterial challenge. Fish Shellfish Immunol. 81, 73–82. https://doi.org/10.1016/j.fsi.2018.07.010

Cima, F., Matozzo, V., Marin, M.G., Ballarin, L., 2000. Haemocytes of the clam *Tapes philippinarum* (Adams & Reeve, 1850): morphofunctional characterisation. Fish Shellfish Immunol. 10, 677–693. https://doi.org/10.1006/fsim.2000.0282

Coen, L.D., Bishop, M.J., 2015. The ecology, evolution, impacts and management of host–parasite interactions of marine molluscs. J. Invertebr. Pathol. 131, 177–211. https://doi.org/10.1016/j.jip.2015.08.005

Comesaña, P., Casas, S.M., Cao, A., Abollo, E., Arzul, I., Morga, B., Villalba, A., 2012. Comparison of haemocytic parameters among flat oyster *Ostrea edulis* stocks with different susceptibility to bonamiosis and the Pacific oyster *Crassostrea gigas*. J. Invertebr. Pathol. 109, 274–286. https://doi.org/10.1016/j.jip.2011.12.007

Da Silva, P., Comesana, P., Fuentes, J., Villalba, A., 2008. Variability of haemocyte and haemolymph parameters in European flat oyster *Ostrea edulis* families obtained from brood stocks of different geographical origins and relation with infection by the protozoan *Bonamia ostreae*. Fish Shellfish Immunol. 24, 551–563. https://doi.org/10.1016/j.fsi.2007.11.003

da Silva, P.M., Scardua, M.P., Vianna, R.T., Mendonça, R.C., Vieira, C.B., Dungan, C.F., Scott, G.P., Reece, K.S., 2014. Two *Perkinsus* spp. infect *Crassostrea gasar* oysters from cultured and wild populations of the Rio São Francisco estuary, Sergipe, northeastern Brazil. J. Invertebr. Pathol. 119, 62–71. https://doi.org/10.1016/j.jip.2014.04.005

da Silva, P.M., Vianna, R.T., Guertler, C., Ferreira, L.P., Santana, L.N., Fernández-Boo, S., Ramilo, A., Cao, A., Villalba, A., 2013. First report of the protozoan parasite *Perkinsus marinus* in South America, infecting mangrove oysters *Crassostrea rhizophorae* from the Paraíba River (NE, Brazil). J. Invertebr. Pathol. 113, 96–103. https://doi.org/10.1016/j.jip.2013.02.002

Dang, C., Tan, T., Moffit, D., Deboutteville, J.D., Barnes, A.C., 2012. Gender differences in hemocyte immune parameters of bivalves: The Sydney rock oyster *Saccostrea glomerata* and the pearl oyster *Pinctada fucata*. Fish Shellfish Immunol. 33, 138–142. https://doi.org/10.1016/j.fsi.2012.04.007

Dantas Neto, M.P., Maggioni, R., Nogueira, L.F.F., Forte, J.M., Feijó, R.G., Sabry, R.C., 2020. *Perkinsus* sp. infecting three important mollusks from Jaguaribe River estuary, Ceará, Brazil. Brazilian J. Vet. Res. Anim. Sci. 57, e158316. https://doi.org/10.11606/issn.1678-4456.bjvras.2020.158316

de la Ballina, N.R., Maresca, F., Cao, A., Villalba, A., 2022. Bivalve Haemocyte Subpopulations: A Review. Front. Immunol. 13. https://doi.org/10.3389/fimmu.2022.826255

Donaghy, L., Kim, B.-K., Hong, H.-K., Park, H.-S., Choi, K.-S., 2009a. Flow cytometry studies on the populations and immune parameters of the hemocytes of the Suminoe oyster, *Crassostrea ariakensis*. Fish Shellfish Immunol. 27, 296–301. https://doi.org/10.1016/j.fsi.2009.05.010

Donaghy, L., Lambert, C., Choi, K., Soudant, P., 2009b. Hemocytes of the carpet shell clam (*Ruditapes decussatus*) and the Manila clam (*Ruditapes philippinarum*): Current knowledge and future prospects. Aquaculture 297, 10–24. https://doi.org/10.1016/j.aquaculture.2009.09.003

Donaghy, L., Volety, A.K., 2011. Functional and metabolic characterization of hemocytes of the green mussel, *Perna viridis*: *In vitro* impacts of temperature. Fish Shellfish Immunol. 31, 808–814. https://doi.org/10.1016/j.fsi.2011.07.018

Evariste, L., Auffret, M., Audonnet, S., Geffard, A., David, E., Brousseau, P., Fournier, M., Betoulle, S., 2016. Functional features of hemocyte subpopulations of the invasive mollusk species *Dreissena polymorpha*. Fish Shellfish Immunol. 56, 144–154. https://doi.org/10.1016/j.fsi.2016.06.054

Fournier, M., Cyr, D., Blakley, B., Boermans, H., Brousseau, P., 2000. Phagocytosis as a biomarker of immunotoxicity in wildlife species exposed to environmental xenobiotics. Am. Zool. 40, 412–420.

Friebel, B., Renwrantz, L., 1995. Application of density gradient centrifugation for separation of eosinophilic and basophilic hemocytes from *Mytilus edulis* and characterization of both cell groups. Comp. Biochem. Physiol. Part A Physiol. 112, 81–90. https://doi.org/10.1016/0300-9629(95)00086-M

García-García, E., Prado-Alvarez, M., Novoa, B., Figueras, A., Rosales, C., 2008. Immune responses of mussel hemocyte subpopulations are differentially regulated by enzymes of the PI 3-K, PKC, and ERK kinase families. Dev. Comp. Immunol. 32, 637–53. https://doi.org/10.1016/j.dci.2007.10.004

Hégaret, H., Smolowitz, R.M., Sunila, I., Shumway, S.E., Alix, J., Dixon, M., Wikfors, G.H., 2010. Combined effects of a parasite, QPX, and the harmful-alga, *Prorocentrum minimum* on northern quahogs, *Mercenaria mercenaria*. Mar.

Environ. Res. 69, 337–344. https://doi.org/10.1016/j.marenvres.2009.12.008

Hégaret, H., Wikfors, G.H., Soudant, P., 2003. Flow cytometric analysis of haemocytes from eastern oysters, *Crassostrea virginica*, subjected to a sudden temperature elevation. J. Exp. Mar. Bio. Ecol. 293, 249–265. https://doi.org/10.1016/S0022-0981(03)00235-1

Hine, P.M., 1999. The inter-relationships of bivalve haemocytes. Fish Shellfish Immunol. 9, 367–385. https://doi.org/10.1006/fsim.1998.0205

Hong, H.-K., Donaghy, L., Choi, K.-S., 2014. Flow cytometric studies on the morphology and immunological functions of hemocytes in the Iwagaki oyster *Crassostrea nippona*. Fish. Sci. 80, 969–976. https://doi.org/10.1007/s12562-014-0777-z

Hong, H., Kang, H., Le, T.C., Choi, K., 2013. Comparative study on the hemocytes of subtropical oysters *Saccostrea kegaki* (Torigoe & Inaba, 1981), *Ostrea circumpicta* (Pilsbry, 1904), and *Hyotissa hyotis* (Linnaeus, 1758) in Jeju Island, Korea: Morphology and functional aspects. Fish Shellfish Immunol. 35, 2020–2025. https://doi.org/10.1016/j.fsi.2013.09.022

Ittoop, G., George, K.C., Sanil, N.K., George, R.M., Sobhana, K.S., Nisha, P.C., 2006. Characterization of haemocytes of the Indian edible oyster, *Crassostrea madrasensis* (Preston). Aquac. Res. 37, 1636–1643. https://doi.org/10.1111/j.1365-2109.2006.01606.x

Jauzein, C., Donaghy, L., Volety, A.K., 2013. Flow cytometric characterization of hemocytes of the sunray venus clam *Macrocallista nimbosa* and influence of salinity variation. Fish Shellfish Immunol. 35, 716–724. https://doi.org/10.1016/j.fsi.2013.06.003

Lassudrie, M., Hégaret, H., Wikfors, G.H., da Silva, P.M., 2020. Effects of marine

harmful algal blooms on bivalve cellular immunity and infectious diseases: A review. Dev. Comp. Immunol. 108, 103660. https://doi.org/10.1016/j.dci.2020.103660

Li, J., Zhang, Yuehuan, Mao, F., Lin, Y., Xiao, S., Xiang, Z., Ma, H., Zhang, Yang, Yu, Z., 2018. The first morphologic and functional characterization of hemocytes in Hong Kong oyster, *Crassostrea hongkongensis*. Fish Shellfish Immunol. 81, 423–429. https://doi.org/10.1016/j.fsi.2018.05.062

Li, S., Liu, Y., Liu, C., Huang, J., Zheng, G., Xie, L., Zhang, R., 2015. Morphology and classification of hemocytes in *Pinctada fucata* and their responses to ocean acidification and warming. Fish Shellfish Immunol. 45, 194–202. https://doi.org/10.1016/j.fsi.2015.04.006

Liu, J., Zhao, Y., 2018. Morphological and functional characterization of clam *Ruditapes philippinarum* haemocytes. Fish Shellfish Immunol. 82, 136–146. https://doi.org/10.1016/j.fsi.2018.08.019

Luz Cunha, A.C., Pontinha, V. de A., de Castro, M.A.M., Sühnel, S., Medeiros, S.C., Moura da Luz, Â.M., Harakava, R., Tachibana, L., Mello, D.F., Danielli, N.M., Dafre, A.L., Magalhães, A.R.M., P. Mouriño, J.L., 2019. Two epizootic *Perkinsus* spp. events in commercial oyster farms at Santa Catarina, Brazil. J. Fish Dis. 42, 455–463. https://doi.org/10.1111/jfd.12958

Mattila, P.K., Lappalainen, P., 2008. Filopodia: molecular architecture and cellular functions. Nat. Rev. Mol. Cell Biol. 9, 446–454. https://doi.org/10.1038/nrm2406

Nguyen, V.T., Alfaro, A.C., 2019. Applications of flow cytometry in molluscan immunology: Current status and trends. Fish Shellfish Immunol. 94, 239–248. https://doi.org/10.1016/j.fsi.2019.09.008

Parrino, V., Costa, G., Cannavà, C., Fazio, E., Bonsignore, M., Concetta, S., Piccione,

G., Fazio, F., 2019. Flow cytometry and micro-Raman spectroscopy: Identification of hemocyte populations in the mussel *Mytilus galloprovincialis (*Bivalvia: Mytilidae) from Faro Lake and Tyrrhenian Sea (Sicily, Italy). Fish Shellfish Immunol. 87, 1–8. https://doi.org/10.1016/j.fsi.2018.12.067

Prado-Alvarez, M., Romero, A., Balseiro, P., Dios, S., Novoa, B., Figueras, A., 2012. Morphological characterization and functional immune response of the carpet shell clam (*Ruditapes decussatus*) haemocytes after bacterial stimulation. Fish Shellfish Immunol. 32, 69–78. https://doi.org/10.1016/j.fsi.2011.10.019

Preziosi, B.M., Bowden, T.J., 2016. Morphological characterization via light and electron microscopy of Atlantic jackknife clam (*E directus*) hemocytes. Micron 84, 96–106. https://doi.org/10.1016/j.micron.2016.03.003

Queiroga, F.R., Marques-Santos, L.F., Hégaret, H., Soudant, P., Farias, N.D., Schlindwein, A.D., Mirella da Silva, P., 2013. Immunological responses of the mangrove oysters *Crassostrea gasar* naturally infected by *Perkinsus* sp. in the Mamanguape Estuary, Paraíba state (Northeastern, Brazil). Fish Shellfish Immunol. 35, 319–327. https://doi.org/10.1016/j.fsi.2013.04.034

Queiroga, F.R., Vianna, R.T., Vieira, C.B., Farias, N.D., Da Silva, P.M., 2015. Parasites infecting the cultured oyster *Crassostrea gasar* (Adanson, 1757) in Northeast Brazil. Parasitology 142, 756–766. https://doi.org/10.1017/S0031182014001863

Rebelo, M. de F., Figueiredo, E. de S., Mariante, R.M., Nóbrega, A., de Barros, C.M., Allodi, S., 2013. New insights from the oyster *Crassostrea rhizophorae* on bivalve circulating hemocytes. PLoS One 8, e57384. https://doi.org/10.1371/journal.pone.0057384

Renault, T., 2015. Immunotoxicological effects of environmental contaminants on marine bivalves. Fish Shellfish Immunol. 46, 88–93.

https://doi.org/10.1016/j.fsi.2015.04.011

Renault, T., Xue, Q.-G., Chilmonczyk, S., 2001. Flow cytometric analysis of European flat oyster, *Ostrea edulis,* haemocytes using a monoclonal antibody specific for granulocytes. Fish Shellfish Immunol. 11, 269–274. https://doi.org/10.1006/fsim.2000.0312

Rodgers, C., Arzul, I., Carrasco, N., Furones Nozal, D., 2019. A literature review as an aid to identify strategies for mitigating ostreid herpesvirus 1 in *Crassostrea gigas* hatchery and nursery systems. Rev. Aquac. 11, 565–585. https://doi.org/10.1111/raq.12246

Rolton, A., Delisle, L., Berry, J., Venter, L., Webb, S.C., Adams, S., Hilton, Z., 2020. Flow cytometric characterization of hemocytes of the flat oyster, *Ostrea chilensis*. Fish Shellfish Immunol. 97, 411–420. https://doi.org/10.1016/j.fsi.2019.12.071

Rolton, A., Ragg, N.L.C., 2020. Green-lipped mussel (*Perna canaliculus*) hemocytes: A flow cytometric study of sampling effects, sub-populations and immune-related functions. Fish Shellfish Immunol. 103, 181–189. https://doi.org/10.1016/j.fsi.2020.05.019

Sabry, R.C., Gesteira, T.C.V., Magalhães, A.R.M., Barracco, M.A., Guertler, C., Ferreira, L.P., Vianna, R.T., da Silva, P.M., 2013. Parasitological survey of mangrove oyster, *Crassostrea rhizophorae*, in the Pacoti River Estuary, Ceará State, Brazil. J. Invertebr. Pathol. 112, 24–32. https://doi.org/10.1016/j.jip.2012.10.004

Salimi, L., Jamili, S., Motalebi, A., Eghtesadi-Araghi, P., Rabbani, M., Rostami-Beshman, M., 2009. Morphological characterization and size of hemocytes in *Anodonta cygnea*. J. Invertebr. Pathol. 101, 81–85. https://doi.org/10.1016/j.jip.2009.03.003

Scardua, M., Vianna, R., Duarte, S., Farias, N., Correia, M., dos Santos, H., da Silva, P., 2017. Growth, mortality and susceptibility of oyster *Crassostrea* spp. to *Perkinsus* spp. infection during on-growing in northeast Brazil. Rev. Bras. Parasitol. Veterinária 26, 401–410. https://doi.org/10.1590/s1984-29612017061

Valenti, W.C., Barros, H.P., Moraes-Valenti, P., Bueno, G.W., Cavalli, R.O., 2021. Aquaculture in Brazil: past, present and future. Aquac. Reports 19, 100611. https://doi.org/10.1016/j.aqrep.2021.100611

Wang, Y., Hu, M., Li, Q., Li, J., Lin, D., Lu, W., 2014. Immune toxicity of TiO2 under hypoxia in the green-lipped mussel *Perna viridis* based on flow cytometric analysis of hemocyte parameters. Sci. Total Environ. 470–471, 791–799. https://doi.org/10.1016/j.scitotenv.2013.09.060

Xie, Z., Wei, S., Dong, H., Chen, H., Zhang, Q., Liu, W., Peng, J., Sokolova, I.M., Hu, M., Wang, Y., 2021. Hemocyte Responses of the Oyster *Crassostrea hongkongensis* Exposed to Diel-Cycling Hypoxia and Salinity Change. Front. Mar. Sci. 8, 1–17. https://doi.org/10.3389/fmars.2021.749623

Xue, Q.-G., Renault, T., Chilmonczyk, S., 2001. Flow cytometric assessment of haemocyte sub-populations in the European flat oyster, *Ostrea edulis*, haemolymph. Fish Shellfish Immunol. 11, 557–567. https://doi.org/10.1006/fsim.2001.0335

Zeng, Y., Huo, Y., Yang, H., 2021. Immunological assays of hemocytes in the Northern Quahog *Mercenaria mercenaria*. Fish Shellfish Immunol. 118, 261–269. https://doi.org/10.1016/j.fsi.2021.09.006

Zhang, T., Qiu, L., Sun, Z., Wang, L., Zhou, Z., Liu, R., Yue, F., Sun, R., Song, L., 2014. The specifically enhanced cellular immune responses in Pacific oyster (Crassostrea gigas) against secondary challenge with *Vibrio splendidus*. Dev.

Comp. Immunol. 45, 141–150. https://doi.org/10.1016/j.dci.2014.02.015